# Some printing parameters affecting the screw withdrawal strength of materials used in joints developed in 3D printers for furniture

Mesut Uysal[1]* ⓘD

**ABSTRACT:** This study examined to benchmark the screw withdrawal strength (SWS) of the 3D-printed PLA materials considering various infill patterns and ratios. SWS is one of the critical material properties for furniture joints. For this purpose, dimensions of $10 \times 50 \times 50$ mm specimens made of PLA+ were printed according to ASTM D 6117-18. Three infill patterns (line, grid, and concentric) and four infill ratios (25%, 50%, 75%, and 100%) were used as printing parameters to construct a complete $3 \times 4$ factorial experiment. According to the results, line infill patterns had the highest density compared to the grid and concentric patterns for all infill ratios. Concentric infill patterns with an infill ratio of 100% (108.41 MPa) had the greatest SWS. Grid infill patterns provided higher strength at the lower infill ratios than line and concentric infill patterns. Here, diffusion for interfaces of strands affected the SWSs of the 3D-printed materials. This study would provide insight into the 3D-printed joints in the field of furniture mechanics.

**Keywords**: Polylactic acid, 3D printing, Furniture joint, Screw withdrawal strength

# Mobilyalar için 3B yazıcılarda geliştirilen birleştirmelerde kullanılan malzemenin vida tutma kapasitesini etkileyen bazı baskı parametreleri

**ÖZ:** Bu çalışma, çeşitli dolgu desenleri ve oranları dikkate alınarak 3D baskı ile üretilen PLA malzemelerinin vida çekme dayanımını (VÇD) karşılaştırılmasını incelemiştir. VÇD mobilya birleştirmeleri için önemli bir malzeme özelliğidir. Bu amaçla, ASTM D 6117-18 standardına göre $10 \times 50 \times 50$ mm boyutlarında numuneler basılmıştır. $3 \times 4$ faktörel deney için üretim parametreleri olarak üç dolgu deseni (çizgi, ızgara ve konsantrik) ve dört dolgu oranı (%25, %50, %75 ve %100) kullanılmıştır. Çalışma sonuçlara göre, çizgi dolgu desenleri, tüm dolgu oranlarında ızgara ve konsantrik desenlere kıyasla en yüksek yoğunluğa sahip olmuştur. %100 dolgu oranına sahip konsantrik dolgu desen en yüksek VCD'na sahiptir (108,01 MPa). Düşük dolgu oranlarında ise ızgara dolgu desenleri, çizgi ve konsantrik dolgu desenlerine göre daha yüksek dayanım sağlamıştır. Burada, ipliklerin arayüzleri için oluşan difüzyon 3B baskılanan malzemelerin VDÇ'lerini etkilemektedir. Bu çalışma, mobilya mekaniği alanında 3B baskı ile üretilen birleştirmelere dair öngörüler sunacaktır.

**Anahtar kelimeler**: Polilaktik asit, 3B yazdırma, Mobilya birleştirme, Vida tutma kapasitesi

## 1    Introduction

3D printing, also called additive manufacturing (AM), has brought recent opportunities to produce parts/products with high precision in digital design manufacturing. Initially used for rapid prototyping, it now encompasses various applications from aerospace to medical devices. Manufactured parts/products are easy to operate and assemble in their final products. Likewise, the popularity of 3D printing technology has evolved significantly in the manufacture of plastic-based furniture joints in the furniture industry.

3D-printed joints for furniture have recently been interesting in examining their strength. Aiman et al. (2020) developed a joint for modular furniture and stated that PETG provided a higher strength joint than ABS, and the design geometry of the joint was effective on joint strength. Nicolau et al. (2022) compared the strength of wooden mortise, tenon (MT) and 3D-printed three-dimensional joints. MT joints had higher strength by 47% and 133% than 3D-printed joints in tension and compression, respectively. Changes in joint design and raster orientation in 3D printing were suggested for higher strength. Nicolau and Çoşeranu (2024) changed the design of joints, and 3D-printed joint strength in tension was higher by 30% than MT joints made of beech wood, but those of compression were lower by 23%. Development of L- or T-shaped joint design in additive manufacturing via fused deposition modeling (FDM) method may not provide intended strength because raster orientation for strands is 90°/90° in the transition from horizontal to the vertical stipe. Hajdarevic et al. (2023) showed that failure occurred at the transition from vertical to horizontal stripe with discontinuities in the layers. Therefore, a single-direction furniture joint with 0°/0° raster orientation (through the length of the joint) and developing its self-locking system may provide sufficient strength. Smardzewski et al. (2016) developed dual-conical joints for modular furniture. Demirel et al. (2024) compared the strength of the 3D-printed dowel joints with different surface patterns and found that joint strength with 3D-printed was not significantly different from that of wood dowels. In order to increase joint strength with dowels, auxetic dowels for furniture joints were developed and their experimental and numerical results were discussed (Kasal et al., 2020, Kuşkun et al., 2021 & Kasal et al., 2023). Newly developed invisible and self-locking system joints were developed by Krzyaniak and Smardzewski (2019), Podskarbi and Smardzewski (2019) and Krzyaniak et al. (2021). The studies mentioned above showed that 3D-printed joints could provide sufficient strength for the furniture. However, in some cases, FDM method may not provide high-precision printing for models such as fine-threaded fasteners. Hence, using metal fasteners for joint–to-joint and joint-to-member assembly could be an intermediate method.

Feng et al. (2020) developed bistable joints and used connectors with short-treated bolts to fasten joints and plastic pipe furniture elements. Even though material strength for 3D-printed furniture joints has been investigated, such as tensile and bending properties, their screw withdrawal strength (SWS) has not been investigated since screws play a critical role in self-locking systems in furniture joints. However, it was discussed for wood plastic composite materials (Haftkhani et al., 2011 & Ghanbari et al., 2014). In order to provide sufficient strength in furniture joints, the properties of materials such as wood-plastic composites, wood-based composites and solid wood come to the fore. The performance and quality of 3D-printed parts are highly dependent on the optimization of several printing parameters. Layer height or the thickness of each printed layer and width are crucial parameters in determining the printed resolution of an object and surface finish. The higher layer thickness results in lower material strength owing to the greater distance between the nozzle and deposited material during extrusion, correspondingly, it causes lower pressure. Besides, greater layer thickness reduces the cooling time of the material, so layers adhere inadequately to each other

(Wang et al., 2020). Optimization of layer height involves balancing the desired resolution with practical constraints such as print speed and material properties. While the layer height can be assigned in the slicing of the 3D model, layer width is regarding to nozzle die and diameters for material flow. Sharma et al. (2021) stated that nozzle dies with various shapes (circular, rectangular, etc.) provide faster prototyping and printing of plant-based materials for large-scale and complex products.

The infill ratio refers to the amount of material used inside the printed part. Higher infill ratios increase the strength and durability of the part and increase material consumption and print time. Lower infill ratios reduce material usage and printing time but may compromise the structural integrity of the parts (Alvarez et al., 2016). The choice of infill ratio depends on the application requirements and the desired balance between strength and material efficiency. Bardiya et al. (2021) highlighted that the highest flexural strength was obtained for the parameters of 0,3 mm layer thickness, 30º raster orientation, and 80% infill ratio while those of tensile were 0.2 mm, 30º, and 80%, respectively. Evlen et al. (2019) stated that increasing the infill ratio from 10% to 30% enhanced material strength by 38% while those of 30% to 50% were 32%. In a tensile test, the increase in the infill ratio from 15% to 50% and 50% to 100% were 18.53% and 59.80%, respectively. Those of ABS were 28.05% and 45.73% (Öz et al., 2018). It can be said that an increase in the infill ratio does not result in a linearly proportional increase in material strength. Infill ratio was the most particular parameter compared to the infill pattern and nozzle temperature (Zurnacı, 2023). Kam et al. (2019) examined the effects of the infill patterns on the tensile strength of the 3D-printed PETG and concluded that the rectilinear pattern had the highest strength followed by triangular, grid, and honeycomb.

Temperature control is vital in 3D printing affecting material flow and adhesion. Different materials require different extrusion temperatures to achieve optimal performance. For example, PLA typically prints at lower temperatures compared to ABS. Inconsistent temperature can lead to issues such as warping, poor layer adhesion or stringing. On the other hand, the material is almost liquid and partially thermally degraded if the nozzle temperature is too high (Sin et al., 2013 & Re et al., 2014). If applicable, proper calibration of the hot end and heated bed is essential for optimal print quality. Wang et al. (2020) stated that an increase in temperature from 195 ºC to 210 ºC improved the material strength. Still, an increase in temperature from 210 ºC to 220 ºC slightly changed them. However, there was a dramatic reduction in elongation at the break because fragility was increased due to thermal degradation. Similarly, Premphet et al. (2023) observed a dramatic decrease in compression strength of 3D-printed PLA with an increase in the nozzle temperature from 215 ºC to 235 ºC. In PLA, yield strength in the tensile test was the highest at the temperature of 215ºC followed by 210 ºC and 190 ºC, and the lowest at 200 ºC. Aydın et al. (2019) observed that the tensile strength of 3D-printed PLA was greater with the increase in temperature from 190 ºC to 220 ºC, but lower with the increase in printing speed from 30 mm/s to 70 mm/s.

The choice of material significantly impacts the final properties of the products. Common materials include PLA, ABS, PETG, and more advanced composites. Each material has its own set of printing parameters and characteristics such as melting temperature, flexibility, and strength. The material selection should align with the desired mechanical properties and functionality of the printed part. Kamer et al. (2021) observed that nozzle and bed temperatures affected the flexural strength of 3D-printed ABS by 15% but did not significantly affect the results. Besides, changes in bed temperatures did not significantly affect the material strength of 3D-printed PLA. Still, a decrease in nozzle temperature dramatically decreased its flexural strength due to low ductility/higher fragility. Filament

color significantly affected the percent crystallinity of material due to ingredients in their color pigment (Wang et al., 2020).

This study aims to investigate various infill patterns and ratios on the SWS of the 3D-printed materials. In doing so, three infill patterns; namely, line, grid and concentric, and four infill ratios (25%, 50%, 75% and 100%) were examined. In doing so, it would be provided an insight the selection of infill ratio to reduce material cost and printing time, and infill pattern to provide sufficient strength in the case of the use of screws in the furniture joint.

## 2 Material and Method

### 2.1 Material

In this study, PLA+ filament was used. PLA is the most preferable material in furniture joints and bioplastic/biodegradable polymer to print in the FDM, a renewable resource derived from corn sugar, potato, and sugar cane (Drumright et al., 2000). Some properties of the filament used in the study are given in Table 1. A DIN 45 3.5 × 45 mm particleboard screws were used.

**Table 1.** Some properties of the PLA+ filaments (URL – 1)

| Density | Tensile Strength | Flexural Strength | Flexural Modulus | Heat Distortion Temperature | Melt Flow Index |
|---|---|---|---|---|---|
| 1.23 g/cm$^3$ | 63 MPa | 74 MPa | 1973 MPa | 53ºC | 5 (190 ºC/2.16 kg) |

### 2.2 Method

#### 2.2.1 3D printing

All samples were modeled on AutoCAD 2025 with dimensions of 10 × 50 × 50 mm according to ASTM D6117 18 (2016). Sample thickness was selected as 10 mm because samples depart from the platform at 100% infill ratio due to thermal conductivity. The models were sliced on Creality Slicer 4.8 software to establish printing parameters. Printing parameters are given in Table 2. The infill ratios and patterns are given in Figure 1. All samples were printed on a Creality Ender-3 V2 Neo 3D printer (Figure 2).

**Table 2.** Printing parameters used in slicing of the specimen

| Parameters | Description |
|---|---|
| Nozzle temperature | 220 °C |
| Bed temperature | 60 °C |
| Nozzle diameter | 0.4 mm |
| Layer thickness | 0.3 mm |
| Flow rate | 100% |
| Printing speed | 50 mm/min |
| Raster orientation | 0°/0° |
| Number of wall layers | 2 |
| Number of top/bottom layers | 2 |
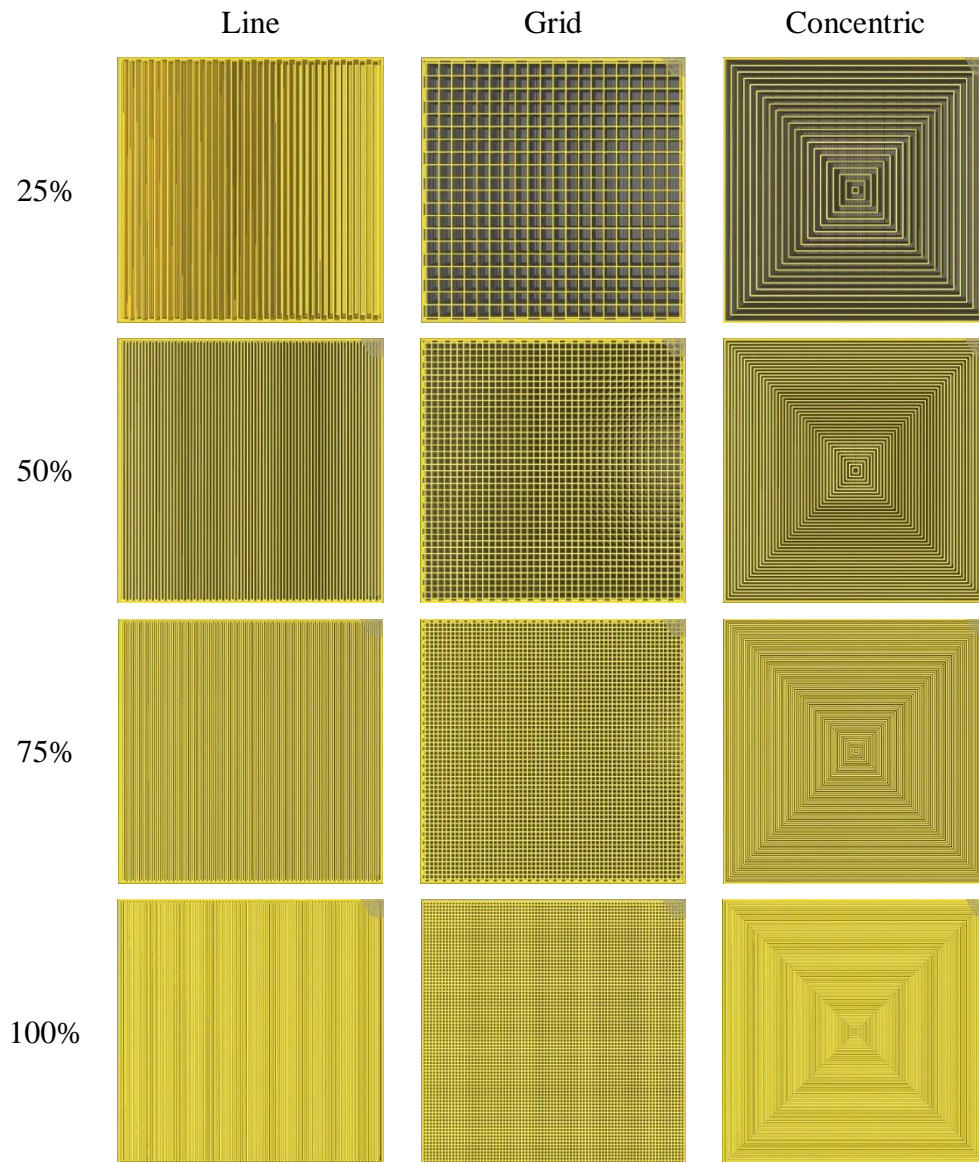
**Figure 1.** Infill ratio and patterns used in the study
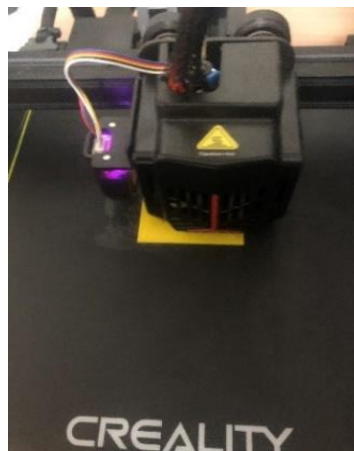


**Figure 2.** 3D printing for specimens.

### 2.2.2   Sample Preparation

All samples were drilled for a pilot hole with a diameter of 2.80 mm at the center of the specimens (Figure 3a). Then, $3.5 \times 45$ mm screws were screwed until at least three teeth protruded to ensure that the full-diameter of the screws was embedded in the pilot hole (Figure 3b). This study examines three infill patterns and four infill ratios, correspondingly, twelve sample groups. Five specimens were replicated in each sample group.



| (a) | (b) |
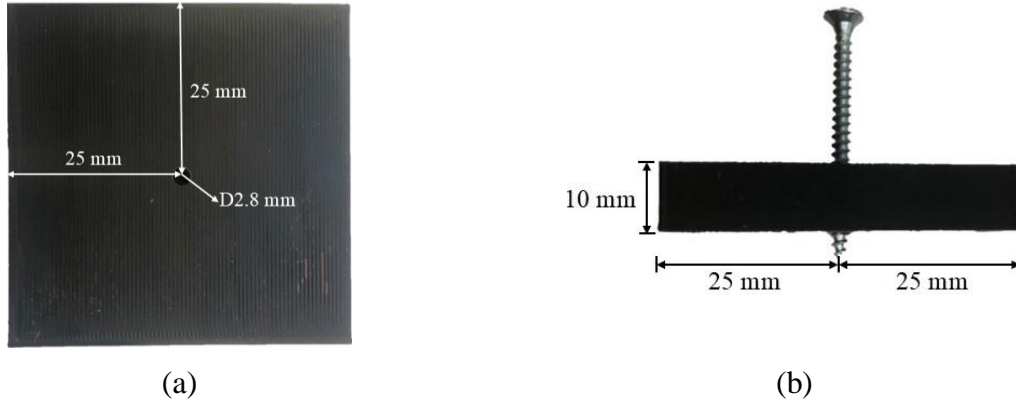
**Figure 3.** Pilot hole diameter and position (a) and configuration of drilled specimen (b)

### 2.2.3   Density

A total of five test specimens for each sample group with dimensions of 10 x 50 x 50 were used to measure the density of the 3D-printed specimens. All specimens were weighed with a 0.01 gr precision scale. Its dimensions were measured with a 0.01 precision caliper. The density ($\rho$, kg/m$^3$) of the 3D-printed specimens was calculated by using Equation 1.

$$\rho = \frac{m}{V} \tag{1}$$

where, $m$ is the weight of the specimen (kg), and $V$ is the volume of the specimen (m$^3$).

### 2.2.4   Screw withdrawal strength

All tests were conducted on the SHIMADZU universal test machine with a rate of 2.5 mm/min according to ASTM D6117 18 (2016) (Figure 4). All tests were continued until non-recoverable failure occurred. Load-deformation curves were obtained, and the SWS (*f*, MPa) of the specimens was calculated by using Equation 2.

$$f = \frac{F_{ult}}{d \times l_p} \tag{2}$$

where, $F_{ult}$ is the ultimate failure load (N), $d$ is the screw diameter (mm), and $l_p$ is the depth of penetration (mm).
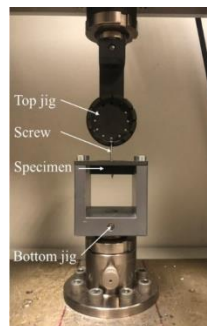


**Figure 4.** Screw withdrawal test configuration.

### 2.2.5 Statistical analysis

Data collected for the presence of statistical significance among all sample groups through two-way ANOVA and Tukey pair-wise comparisons were examined in SPSS (22, New York, USA).

## 3 Results and Discussion

### 3.1. Density of 3D-printed materials

Results for densities of 3D printed specimens with various infill ratios and patterns were given in Table 3. According to the results, an increase in infill ratios is expected to increase the density of the specimens. The average densities of the specimens with the infill ratios of 25%, 50%, and 75% were approximately 39%, 60%, and 81% of those of 100%, respectively. Besides, although the density of the PLA+ filament is 1230 kg/m$^3$, the average densities of specimens for all infill patterns with infill ratios of 100% were lower due to porosity in 3D printing. The ratios between them were 93.07%, 92.31%, and 92.15% for the line, grid, and concentric infill patterns, respectively. It can be said that infill patterns slightly changed the porosity in 3D printing. Besides, Table 3 shows the Tukey-pairwise mean comparisons considering infill patterns and ratios for densities. According to the results, average densities of 3D-printed specimens with an infill ratio of 100% were not significantly different from each other regardless of infill patterns. The same situation was valid for those of 75%. Moreover, average densities were not significantly different in line and grid infill patterns with an infill ratio of 25% and 50%. Here, needless to say that the densities did not change depending on infill patterns in the case of printing with infill ratios of 75% and 100%. Besides, it did not matter on densities with decreasing infill ratios which infill patterns were used for line and grid.

**Table 3.** Sample statistics for densities of 3D-printed specimens (kg/m$^3$)

| Infill Ratios | Infill Patterns | | | | | | | | |
|---|---|---|---|---|---|---|---|---|---|
| | Line | | | Grid | | | Concentric | | |
| | Mean | SD | CoV | Mean | SD | CoV | Mean | SD | CoV |
| 25% | 452.90 (B) | 3.40 | 0.75% | 453.00 (B) | 3.17 | 0.70% | 425.98 (A) | 2.31 | 0.54% |
| 50% | 697.35 (D) | 3.26 | 0.47% | 697.47 (D) | 2.40 | 0.34% | 682.03 (C) | 5.66 | 0.83% |
| 75% | 937.67 (E) | 2.79 | 0.30% | 929.56 (E) | 5.46 | 0.59% | 930.97 (E) | 10.04 | 1.08% |
| 100% | 1144.88 (F) | 4.20 | 0.37% | 1135.47 (F) | 4.57 | 0.40% | 1133.46 (F) | 11.10 | 0.98% |

*\* SD: Standard deviation and CoV: Coefficient of variation*
*\*\* Letters in parenthesis show that means significantly different from each other when letters are not same.*

Table 4 shows the results of two-way ANOVA. According to the results, infill pattern, infill ratio, and their interaction were significant in the density of 3D-printed specimens. Besides, variations in infill patterns and ratios explained 100% of changes in the density of the specimens.

**Table 4.** ANOVA for densities of 3D-printed specimens

| Source | Sum of Squares | df | Mean Square | F-value | Sig. |
|---|---|---|---|---|---|
| Corrected Model | 4056400.75 | 11 | 368763.70 | 11788.15 | .000 |
| Intercept | 38565971.44 | 1 | 38565971.44 | 1232825.92 | .000 |
| Infill Pattern (A) | 2414.86 | 2 | 1207.43 | 38.60 | .000 |
| Infill Ratio (B) | 4052628.85 | 3 | 1350876.28 | 43183.02 | .000 |
| A * B | 1357.04 | 6 | 226.17 | 7.23 | .000 |
| Error | 1501.56 | 48 | 31.28 | | |
| Total | 42623873.75 | 60 | | | |
| Corrected Total | 4057902.31 | 59 | | | |
| R-Squared = 1.000 (Adjusted R-Squared = 1.000) | | | | | |

### 3.2. Screw withdrawal strength of 3D-printed materials

Figure 5 gives the ultimate load capacity of 3D-printed PLA specimens and deformations at ultimate load in the screw withdrawal test. According to the results, no matter which infill pattern is used in the specimens, deformations at the ultimate load were scattered for the infill ratios of 25%. This scattered pattern was observed for concentric infill patterns with an infill ratio of 50%. It was evitable that the effective areas of the screw in the withdrawal test were not dense but had a holding capacity. Hence, the specimens failed at the earlier load levels but reached their ultimate load level at greater deformations. The grid infill patterns showed a ladder effect with increases in the infill ratio which was more expected to be observed.
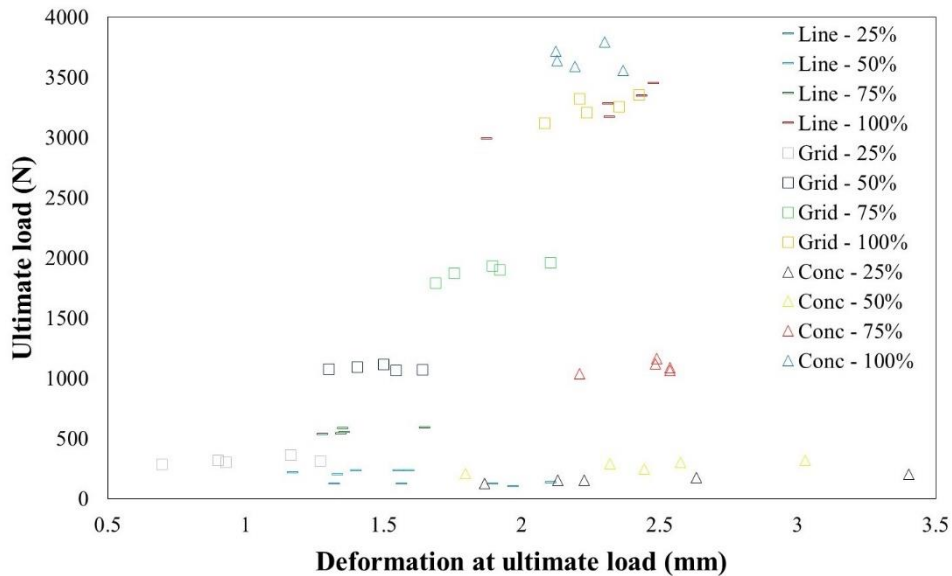


**Figure 5.** Ultimate screw withdrawal load vs. deformation

Results for SWS of 3D-printed PLA specimens are given in Figure 6. According to the results, the highest SWS (108.41 MPa) was obtained for the sample group of concentric infill patterns with a 100% infill ratio followed by line (99.12 MPa) and grid (96.82MPa) infill patterns. On the contrary, grid infill patterns with ratios of 25%, 50%, and 75% had higher strength compared to those of line and concentric. In the infill ratios with 100%, the difference between densities for each infill pattern is close to each other. However, the density in the center of specimens for concentric infill patterns would be higher than those of line and

grid due to the printing path. In the concentric infill patterns, the printing path was from outside to inside, so printers extruded the strand in the shape of smaller squares through the inner section, and these squares caused denser (or less porosity) in the inner part of specimens owing to overlapping strands. On the other hand, grid infill patterns with an infill ratio of 100% had a higher porosity compared to others due to the meshing arrangement in the patterns (Figure 1). On the other hand, this meshing arrangement provided higher SWS in the infill ratios of 25%, 50%, and 75% than those of the line and grid. The dramatic increase in material strength with an infill ratio of 100% was observed by 92% with an increase from 80% to 100% infill ratios (Wang et al., 2020).

Increases in withdrawal resistance of 3D-printed PLA with line infill pattern were approximately twice for 25% to 50% and 50% to 75 % infill ratios while those of 75% to 100% were fifth times. In the case of grid patterns, these increases were about a third, one-and-half, and one-and-three-quarter time, respectively. Those of concentric infill patterns were one-and-half, fourth, and three-and-one-quarter time. Here, it can be said that the increase in the infill ratios did not influence the SWS proportionally. As shown in Figure 1, strands were printed in one (x) direction for line infill patterns, but those of grid and concentric were in two (x and y) directions. In the lower infill ratios, screws were surrounded by strands in the grid and concentric infill patterns, so their SWS were higher than the line infill patterns. Similarly, grid infill patterns were higher in strength compared to those of concentric because strands were printed in a meshing arrangement in grid infills, whereas interfaces of the adjacent strands did not diffuse each other in the lower infill ratios. At the higher infill ratios, the interfaces of the strands diffused vastly, so the SWS of the specimen was dramatically increased. Therefore, the SWS of the specimens with grid infill ratios linearly increased with the higher infill ratios. However, voids in 3D printing observationally had a higher ratio for grid infill patterns compared to those of line and concentric with an infill ratio of 100% (Figure 1). Also, grid infill patterns showed higher material strength owing to linear structure compared to other infill patterns such as triangular and gyroid (Ambati and Ambatipudi, 2022), honeycomb and gyroid (Birosz et al., 2022), and hexagonal and triangular (Khalid et al., 2023) with infill patterns lower than 100%.
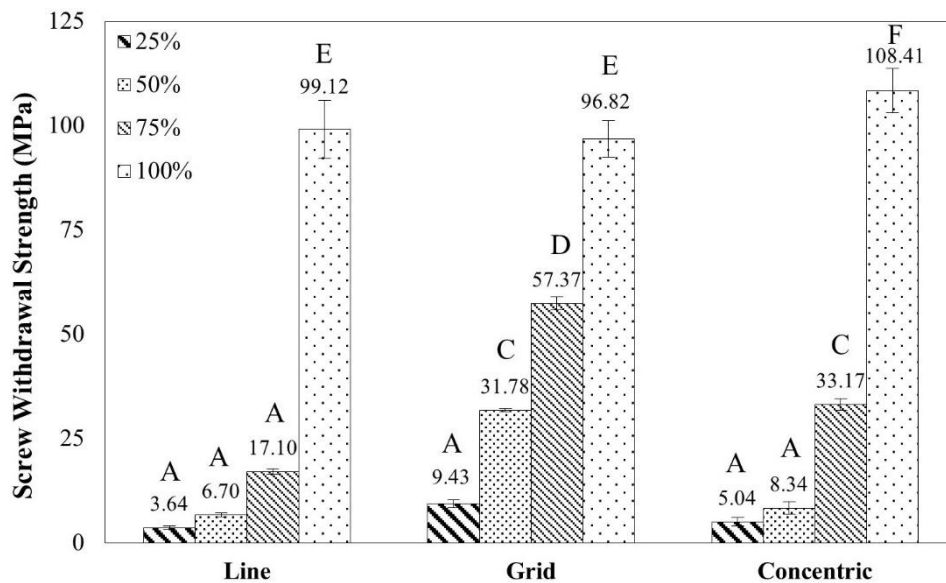


*\* Letters above bars show that means significantly different from each other when letters are not same.*

**Figure 6.** Screw withdrawal strength of the 3D-printed specimens

Moreover, Figure 6 also shows the Tukey-pairwise mean comparisons considering infill patterns and ratios for the SWS. According to the results, the SWS of the 3D-printed specimen with concentric infill patterns and an infill ratio of 100% were significantly different from others. In addition, those of grid and line were not significantly different from each other. The grid infill patterns were significantly different from those of line and concentric in the 50% and 75% infill ratios. The results also indicated that the SWS of the specimen with a grid infill pattern and an infill ratio of 50% was not significantly different from those of concentric and 75%. Here, it can be said that grid infill patterns showed better performance than line and concentric with lower infill ratios than 100%.

Table 5 shows variance analysis for SWS of the 3D-printed specimens. According to the results, (i) infill pattern, (ii) infill ratio, and (iii) interaction of infill pattern and ratio were significant on the SWS of the specimens. Besides, variations in infill patterns and ration explained 99.4% of changes in the SWS of the specimens.

**Table 5.** ANOVA for screw withdrawal strength of the 3D-printed specimens

| Source | Sum of Squares | df | Mean Square | F-Value | Sig. |
|---|---|---|---|---|---|
| Corrected Model | 89669.65 | 11 | 8151.79 | 928.41 | .000 |
| Intercept | 94770.97 | 1 | 94770.97 | 10793.49 | .000 |
| Infill pattern (A) | 2992.53 | 2 | 1496.27 | 170.41 | .000 |
| Infill ratio (B) | 83122.85 | 3 | 27707.62 | 3155.63 | .000 |
| A * B | 3554.26 | 6 | 592.38 | 67.47 | .000 |
| Error | 421.46 | 48 | 8.78 | | |
| Total | 184862.07 | 60 | | | |
| Corrected Total | 90091.11 | 59 | | | |
| R-Squared = .995 (Adjusted R-Squared = .994) | | | | | |

## 4 Conclusion

This study examined to benchmark the SWS of the 3D printed PLA materials considering various infill patterns and ratios. Results showed that infill patterns and ratios significantly affected the SWS of the 3D-printed PLA. According to the study results,

- Infill ratio was a more effective 3D-printing parameter than infill patterns because it provided denser materials which were a significant variable for the SWS of materials.
- In the lower infill ratios (i.e. 25% and 50%), grid infill patterns provided greater strength compared to line and concentric infill patterns because of mesh arrangement during 3D printing extrusion on the path. Therefore, grid infill patterns should be used unless an infill ratio of 100% is preferred in 3D printing.
- The SWS of the specimens with the infill ratio of 100% was improved with increases in density in the effective region of the screw during withdrawal. The printing paths were getting closer to each other in the core of specimens because the ratio of overlapped strands was increased. This phenomenon was observed for the concentric infill patterns.
- The study will give an insight into the field of furniture strength design because most of the studies have been related to determining flexural and tensile properties of 3D-printed materials. Metal fasteners are commonly used in furniture joints. Therefore, the results of this study come into prominence for 3D-printed and screwed furniture joints.

**References**

Aiman, A.F., Sanusi, H., Haidiezul, A.H.M., & Cheong, H.Y., (2020). Design and structural analysis of 3D-printed modular furniture joints, IOP Conf. Series: Material Science and Engineering, 932, 012101, DOI: 10.1088/1757-899X/932/1/012101

Alvarez, K.L., Lagos, R.F., & Aizpun, M., (2016). Investigating the influence of infill percentage on the mechanical properties of fused deposition modelled ABS parts, *Ingeniería e Investigación*, 36 (3), 110-116, DOI: 10.15446/ing.investig.v36n3.56610

Ambati, S.S., & Ambatipudi, R., (2022). Effect of infill density and infill pattern on the mechanical properties of 3D printed PLA parts, *Materials Today: Proceedings*, 64, 804-807, DOI: 10.1016/j.matpr.2022.05.312

ASTM D 6117-18 (2016). Standard test methods for mechanical fasteners in plastic lumber and shapes, ASTM International, West Conshohocken, PA.

Aydın, M., Yıldırım, F. & Çantı, E., (2019). Farkli yazdırma parametrelerinde PLA filamentin işlem performansının incelenmesi, *International Journal of 3D Printing technologies and Digital Industry*, 3(2), 102-115.

Bardiya, S., Jerald, J., & Satheeshkumar, V., (2021). The impact of process parameters on the tensile strength, flexural strength and the manufacturing time of fused filament fabricated (FFF) parts, *Materials Today: Proceedings*, 39, 1362-1366, DOI: 10.1016/j.matpr.2020.04.691

Birosz, M.T., Ledenyak, D., & Ando, M., (2022). Effect of FDM infill patterns on mechanical properties, *Polymer Testing*, 13: 107654, DOI: 10.1016/j.polymertesting.2022.107654

Demirel, S., Kuvel, N.T., Çava, K. & Aslan, M. (2024). The performance of 3D printed dowel with three different surface designs in furniture joints, *Turkish Journal of Forestry*, 25 (1): 100-106, DOI: 10.18182/tjf.1387389

Drumright, R.E., Gruber, P.R., & Henton, D.E., (2000). Polylactic acid technology, *Advanced Materials*, 12(23), 1841-1846.

Evlen, H., Erel, G. & Yılmaz, E., (2018). 3D printer design and investigation of effects on the mechanical properties of the printing fill rates, *International Journal of 3D Printing technologies and Digital Industry*, 2(1), 23-31.

Feng. S., Du, M. Wang, W., Lu, H., Park, D. & Ji, G., (2020). 3D printed monolithic joints: A mechanically bistable joint, 25th International Conference of the Association for Computer-Aided Architectural Design Research in Asia, Bangkok, Thailand, 5-6 August 2020, pp. 173-182, DOI: 10.52842/conf.caadria.2020.1.173

Ghanbari, A., Madhoushi, M., & Ashori, A., (2014). Wood plastic composite panels: influence of the species, formulation variables and blending process on the density and

withdrawal strength of fasteners, *Journal of Polymers and the Environment*, 22, 260-266, DOI: 10.1007/s10924-013-0634-7

Haftkhani, A.R., (2011). Investigation on withdrawal resistance of various screws in face and edge of wood-plastic composite panels, *Materials and Design*, 32, 4100-4106, DOI: 10.1016/j.matdes.2011.02.065

Hajdarevic, S., Kuzman, M.K., Obucina, M., Vratusa, S., Kusar, T., & Kariz, M., (2023). Strength and stiffness of 3D-printed connectors compared with the wooden mortise and tenon joints for chairs, *Wood Material Science & Engineering*, 18(3), 870-883, DOI: 10.1080/17480272.2022.2086065

Kam, M., Saruhan, H., & İpekçi, A., (2019). Effect of filling structures on strength of printed products by 3D printers, *Duzce University Journal of Science and Technology*, 7, 951-960, DOI: 10.29130/dubited.452907

Kamer, M.S., Doğan, O., Temiz, Ş., & Yaykaşlı, H., (2021). Investigation of the mechanical properties of flexural test samples produced using different printing parameters with a 3D printer, *Çukurova University Journal of the Faculty of Engineering*, 36(3), 835-846, DOI: 10.21605/cukurovaumfd.1005909

Kasal, A., Kuşkun, T. & Smardzewski, J., (2020). Experimental and numerical study on withdrawal strength of different types of auxetic dowels for furniture joints, *Materials*, 13(19), 4252, DOI: 10.3390/ma13194252

Kasal, A., Smardzewski, J., Kuşkun, T. & Güray, E., (2023). Analyses of L-type corner joints connected with auxetic dowels for case furniture, *Materials*, 16(13), 4547, DOI: 10.3390/ma16134547

Khalid, J., Gurrapu, D.R., & Elfakhri, F., (2023). Effects of infill line multiplier and patterns on mechanical properties of lightweight and resilient hollow section products manufactured using fused filament fabrication, *Polymers*, 15, 2585, DOI: 10.3390/polym15122585

Krzyzaniak, L., & Smardzewski, J., (2019). Strength and stiffness of new designed externally invisible and demountable joints for furniture cases, *Engineering Structures*, 199, 109674, DOI: 10.1016/j.engstruct.2019.109674

Krzyzaniak, L., Kuşkun, T., Kasal, A., & Smardzewski, J., (2021). Analysis of the internal mounting forces and strength of newly designed fastener to joints wood and wood-based panels, *Materials*, 14(23), 7119, DOI: 10.3390/ma14237119

Kuşkun, T., Smardzewski, J. & Kasal, A., (2021). Experimental and numerical analysis of mounting force of auxetic dowels for furniture joints, *Engineering Structures*, 226, 111351, DOI: 10.1016/j.engstruct.2020.111351

Nicolau, A., Pop, M.A., & Coşereanu, C., (2022). 3D Printing Application in Wood Furniture Components Assembling, *Materials*, 15, 2907, DOI: 10.3390/ma15082907

Nicolau, A., & Coşereanu, C., (2024). Mechanical properties of L-type corner joints connected with 3D printed connectors using fused deposition modelling technology, *Pro Lig*no, 20(2), 69-76.

Öz, Ö., Aydın, M., Kara, A.S., & Sancak, M.S., (2018). Determination of the infill ratio effect on the failure loads of the printed parts, *International Journal of 3D Printing technologies and Digital Industry*, 2(1), 32-39.

Podskarbi, M. & Smardzewski, J., (2019). Numerical modelling of new demountable fasteners for frame furniture. *Engineering Structures*, 185, 221-229, DOI: 10.1016/j.engstruct.2019.01.135

Premphet, P., leksakul, K., Boonyawan, D., & Vichiansan, N., (In Press). Process parameters optimization and mechanical properties of 3D PLA/HA printing scaffold, Materials Today: Proceedings, DOI: 10.1016/j.matpr.2023.04.124

Re, G.L., Benali, S., Habibi, Y., Raquez, J.M., & Dubois, P., (2014). Stereocomplexed PLA nanocomposites: from *in situ* polymerization to materials properties, *European Polymer Journal*, 54, 138-150, DOI: 10.1016/j.eurpolymj.2014.03.004

Sharma, V., Roozbahani, H., Alizadeh, M., & Handross, H., (2021). 3D printing of plant-derived compounds and proposed nozzle design design for the more effective 3D FDM printing, *IEEE Access*, 9(3), 57107-57119, DOI: 10.1109/ACCESS.2021.3071459

Sin, L.T., Rahmat, A.R., & Rahman, W.A., (2013). Thermal Properties of Poly (Lactic Acid) in Polylactic Acid: PLA Biopolymer Technology and Applications, Elsevier, Amsterdam, Netherlands, pp. 109–141.

Smardzewski, J., Rzepa, & Kılıç, H., (2016). Mechanical properties of externally invisible furniture joints made of wood-based composites, Bioresources, 11(1), 1224-1239, DOI: 10.15376/biores.11.1.1224-1239

URL - 1 – eSUN: PLA+. Available online: https://platincdn.com Last access on 10.24. 2024.

Wang, S., Ma, Y., Deng, Z., Zhang, S., & Cai, J., (2020). Effects of fused deposition modeling process parameters on tensile, dynamic mechanical properties of 3D printed polylactic acid materials, *Polymer Testing*, 86, 106483, DOI: 10.1016/j.polymertesting.2020.106483

Zurnacı, E., (2023). Optimization of 3D printing parameters to mechanical strength improvement of sustainable printing material using RSM, *International Journal of 3D Printing technologies and Digital Industry*, 7(1), 38-46, DOI: 10.46519/ij3dptdi.1231076